Explicit Fourier wavefield extrapolators

Gary F. Margrave and Robert J. Ferguson

ABSTRACT

Explicit wavefield extrapolators are based on direct analytic mathematical formulae that express the output as an extrapolation operator acting on the input. Implicit techniques require an equation to be solved, or a matrix decomposed or inverted, to accomplish the extrapolation. Typically, explicit methods are faster and often give more insight into the physics of the wave propagation; but can suffer from instability. Implicit operators are often unconditionally stable.

Four different explicit extrapolators based on Fourier theory are presented and analyzed. They are: PS (ordinary phase-shift), PSPI (phase shift plus interpolation), NSPS (nonstationary phase shift), and, new in this paper, SNPS (symmetric nonstationary phase shift). The PS extrapolator is well known to be exact for constant velocity, unconditionally stable, but inapplicable for variable velocity. PSPI was originally formulated as an interpolation between sets of PS wavefields but it can be formulated as a nonstationary combination filter (or equivalently a pseudodifferential operator). NSPS is similar to PSPI but is a nonstationary convolution filter that gives it different properties. PSPI and NSPS both adapt very rapidly to local lateral velocity changes. When the lateral velocity variation is piecewise constant, NSPS and PSPI reduce to simple operations involving spatial windowing, extrapolation with the PS operator, and superposition. For NSPS, windowing precedes extrapolation while for PSPI it is the reverse.

NSPS and PSPI both lead to analytic expressions for wavefields in heterogeneous media that approximately solve the variable velocity wave equation. Their error terms are fundamentally different in character but vanish for constant velocity.

A formal proof is given that NSPS in a direction orthogonal to the velocity gradient is the mathematical adjoint process to PSPI in the opposite direction. This motivates the construction of SNPS that combines NSPS and PSPI in a symmetric fashion. This symmetry (under interchange of input and output lateral coordinates) is required by reciprocity arguments. PS and SNPS are symmetric while NSPS and PSPI are not.

An extensive numerical stability study using SVD (singular value decomposition) shows that all of these extrapolators can become unstable for strong lateral velocity gradients. Unstable operators allow amplitudes to grow unphysically in a recursion. Stability is enhanced by introducing a small (~3%) imaginary component to the velocities. This causes a numerical attenuation that tends to stabilize the operators but does not address the cause of the instability. For the velocity model studied (a very challenging case) PSPI and NSPS have exactly the same instability while SNPS is always more stable. Instability manifests in a complicated way as a function of extrapolation step size, frequency, velocity gradient, and strength of numerical attenuation. The SNPS operator can be stabilized over a wide range of conditions with considerably less attenuation than is required for NSPS or PSPI.

INTODUCTION

Wavefield extrapolation methods are often categorized as either explicit or implicit. Explicit techniques are those which give a direct mathematical form for the extrapolation operator while implicit methods prescribe an equation which must be solved (numerically) to determine the extrapolated wavefield. Both forms are familiar from finite difference solutions to the wave equation as pioneered by Claerbout (1976). Explicit solutions are valued for their direct simplicity and are often quick to calculate; however, they are often *unstable*. In this context, a stable wavefield extrapolator is one that controls the amplitude of the extrapolated wavefield under recursive application. In a wavefield marching scheme, the wavefield after n steps can be represented as $L^n(\psi_o)$ where ψ_o is the initial wavefield and L^n represents n applications of a (linear) extrapolator. The number of steps is often very large (thousands) and an extrapolator that allows even a small percentage of unphysical growth with each step can lead to wildly uncontrolled amplitudes. Implicit schemes are often formulated to provide a perfectly stable extrapolator but can be difficult to implement efficiently due to the need to solve a set of linear equations at each step.

The prototypical explicit extrapolator is the phase-shift extrapolator of Gazdag (1978). This method, which is exact for constant velocity scalar waves, proceeds with a forward Fourier transform of the input wavefield, then a phase-shift operator is applied, and the result is inverse Fourier transformed. Symbolically, this is

$$\psi(x,z)_{PS} = \underset{k_x \Rightarrow x}{\mathbf{IFT}}\left[\underset{x' \Rightarrow k_x}{\mathbf{FT}}\left(\psi(x',0)\right)\exp(ik_z z)\right] \tag{1}$$

where FT and IFT are forward and inverse Fourier transforms and $\exp(ik_z z)$ is the wavefield extrapolator. Equation (1) is written for a monochromatic wavefield (a single temporal frequency) and can be extended to broad-band data with a temporal Fourier transform. The vertical wavenumber k_z is computed from the simple dispersion relation

$$k_z = \sqrt{\frac{\omega^2}{v^2} - k_x^2} \tag{2}$$

where ω is temporal frequency and v is the (constant) velocity. This procedure is perfectly stable since the extrapolator has unit magnitude for real k_z and is a decaying exponential otherwise.

For variable velocity, the extrapolator is usually formulated for v(x) only (i.e. $\partial v/\partial z=0$) and vertical velocity variations are addressed through recursion. A typical implementation is done in the ω-x domain and the extrapolator is formulated by expanding $\exp(ik_z z)$ as a power series in k_x and then replacing k_x by $i\partial/\partial x$ (e.g. Berkhout, 1984). A practical implementation terminates the series at some order "m" and the result is an m^{th} order differential operator with variable coefficients (powers of v(x)). Such an operator is then approximated with finite differences.

An alternative to this method is the PSPI (phase-shift plus interpolation) technique of Gazdag and Squazerro (1984). PSPI accomplishes an approximate extrapolation

through v(x) using a suitable set of reference velocities $\{v_j\}$. For each reference velocity, a constant-velocity phase-shift extrapolation is computed and, by interpolating these into a single result, the extrapolation through v(x) is simulated.

Etgen (1994) argued that PSPI is equivalent to an ω-x method with a very long operator and showed that such methods can become unstable in complex velocity settings. He proposed a numerical technique to examine the stability of such extrapolators. Formulating the extrapolator as a square matrix of dimension nx by nx (where nx is the number of discrete spatial locations on a seismic line) he used SVD (singular value decomposition) to compute the singular values of the extrapolation matrix. Stability is indicated by singular values less than unity while any singular value in excess of unity causes instability. Figure 1 is from Etgen's paper and shows an example of an unstable extrapolation through an extreme velocity model. Etgen noted that this is an unusual case and that explicit methods generally behave well.

Wapenaar and Grimbergen (1998) extended this stability analysis to their method of *modal decomposition* for the design of one-way extrapolators (Grimbergen et al, 1998). They argued that much of the instability in the explicit ω-x methods arises because the extrapolation matrix is not symmetric, while reciprocity considerations require that it should be so. They showed that modal decomposition leads to operators which are unconditionally stable. The design of such operators requires an eigenvalue decomposition of the Helmholtz operator and is therefore not explicit.

Margrave and Ferguson (1997) presented an analytic expression for the most accurate form of PSPI, thereby making it a truly explicit method, and also introduced another method called NSPS (nonstationary phase shift). PSPI and NSPS were shown to be complementary forms of nonstationary filters and it was suggested that NSPS might be preferable as it is conceptually similar to Huygen's principle while PSPI is not.

In this paper, we will briefly review PSPI and NSPS and then present a number of new developments. We will show that both PSPI and NSPS build approximate solutions to the variable velocity wave equation but with different error terms. Then, we present a proof that PSPI and NSPS are the mathematical "adjoints" of one another. Specifically, extrapolation with NSPS in a given direction is the adjoint of extrapolation with PSPI in the opposite direction (and vice-versa). This result has implications for stability and suggests that a self-adjoint (e.g. Hermetian) process might be formulated by combining NSPS and PSPI into a single algorithm. We give an example of this combined algorithm and call it SNPS (of course). Finally we present an SVD stability analysis of these methods for the same velocity model explored by Etgen (1994). We show that NSPS and PSPI have exactly the same degree of instability but that SNPS is dramatically more stable. We show that the incorporation of a small imaginary component of velocity leads to a numerical dispersion that increases the stability of all of theses methods. We present a numerical exploration of the stability behavior of these methods as a function of dz step, frequency, and magnitude of the imaginary component of velocity.

REVIEW OF PSPI AND NSPS

This section is replicated from our paper "Nonstationary filters, pseudodifferential operators, and their inverses" which appears elsewhere in this research report. It is repeated here for convenience. We define two explicit integral operators for wavefield extrapolation and show their complementary nature. The presentation uses the language of nonstationary filters as presented in Margrave (1998).

PSPI defined

The first operator is the logical extension of the phase-shift-plus-interpolation (PSPI) method of Gazdag and Squazerro (1984). PSPI accomplishes an approximate extrapolation through v(x) using a suitable set of reference velocities $\{v_j\}$. For each reference velocity, a constant-velocity phase-shift extrapolation is computed and, by interpolating these into a single result, the extrapolation through v(x) is simulated. Logically, this process can be taken to the limiting case of an "exhaustive set" of references velocities which means $\{v_j\}$ contains an entry for each distinct value of v(x). In this limit, the details of the interpolation process become irrelevant and the PSPI method converges to

$$\psi(x,z)_{PSPI} = \int \varphi(k_x,0)\alpha(k_x,x,z)\exp(-ik_x x)dk_x \tag{3}$$

where $\varphi(k_x,0,\omega)$ is the forward Fourier transform of $\psi(x,0,\omega)$,

$$\varphi(k_x,0) = \int \psi(x,0)\exp(ik_x x)dx, \tag{4}$$

and $\alpha(k_x,x,z)$ is the nonstationary wavefield extrapolator given by

$$\alpha(k_x,x,z) = \exp\left(iz\sqrt{\frac{\omega^2}{v(x)^2} - k_x^2}\right) = \exp\left(izk_z(x)\right). \tag{5}$$

ψ_{PSPI} is a nonstationary combination filter, which equation (3) gives in the mixed form as a generalized inverse Fourier integral. For the remainder of this paper, when the term PSPI is used it will refer to these generalized equations.

NSPS defined

The second wavefield extrapolation operator is the nonstationary convolution "dual" of PSPI as given above. Called nonstationary phase-shift (NSPS) it is given by

$$\varphi(k_x,z)_{NSPS} = \int \psi(x,0)\alpha(k_x,x,z)\exp(ik_x x)dx \tag{6}$$

where $\alpha(k_x,x,z)$ is again given by equation (5) and

$$\psi(x,z)_{NSPS} = \int \varphi(k_x,z)_{NSPS} \exp(-ik_x x)\, dk_x . \tag{7}$$

Notice that NSPS applies $\alpha(k_x,x,z)$ simultaneously with the forward Fourier transform (from x to k_x). In contrast, PSPI applies the same nonstationary wavefield extrapolator with the inverse Fourier transform (from k_x to x).

The windowing analog for PSPI and NSPS

The windowing analog results in very simple expressions for these two extrapolators. It can be derived by assuming that v(x) is piecewise constant with a countable number of segments. If v_j denotes any of the constant velocities, then define the window set $\{\Omega_j\}$ such that $\Omega_j(x)=1$ if $v(x)=v_j$ and is zero otherwise. Then ψ_{PSPI} may be expressed symbolically as from

$$\psi(x,z)_{PSPI} = \sum_j \left\{ \Omega_j \underset{k_x \Rightarrow x}{\mathbf{IFT}} \left[\alpha_j \underset{x' \Rightarrow k_x}{\mathbf{FT}} \left(\psi(x',0) \right) \right] \right\} \tag{8}$$

where α_j is a wavefield extrapolator for constant velocity v_j. Similarly, NSPS becomes

$$\psi(x,z)_{NSPS} = \underset{k_x \Rightarrow x}{\mathbf{IFT}} \left\{ \sum_j \left[\alpha_j \underset{x' \Rightarrow k_x}{\mathbf{FT}} \left(\Omega_j \psi(x',0) \right) \right] \right\} . \tag{9}$$

Notice that the only difference between these expressions is the location of the windows. It is also interesting to compare them to ordinary phase-shift extrapolation as given by equation (1). Figures 2 and 3 illustrate these processes for the case of upward wavefield extrapolation (i.e. wavefield modeling).

PSPI AND NSPS AS APPROXIMATE SOLUTIONS TO THE WAVE EQUATION

It is of interest to examine the magnitude and form of the error terms that arise when the PSPI and NSPS phase-shift integrals (equations 3 and 6) are substituted into the monochromatic scalar wave equation

$$\frac{\partial^2 \psi}{\partial z^2} + \frac{\partial^2 \psi}{\partial x^2} = -\frac{\omega^2}{v^2(x)} \psi . \tag{10}$$

Here it is assumed that the velocity field depends only on the lateral coordinate. For this purpose, we will first reformulate PSPI and NSPS as full space-domain processes rather than as mixed domain.

For PSPI, substitute equations (4) and (5) into (3) to get

$$\psi(x,z)_{PSPI} = \iint \psi(x',0) \exp\left(ik_z(x) z - ik_x \left[x - x' \right] \right) dx' dk_x \tag{11}$$

Similarly, for NSPS we substitute equation (6) into (7) which gives

$$\psi(x,z)_{NSPS} = \iint \psi(x',0)\exp\left(ik_z(x')z - ik_x\left[x - x'\right]\right)dx'dk_x. \qquad (12)$$

Equations (11) and (12) are directly comparable with the only difference being whether k_z depends on the input or output horizontal coordinate. We wish to investigate how well each solves the wave equation (10).

PSPI formulae

To this end, compute the second partial derivative with respect to z and x of the PSPI formula:

$$\frac{\partial \psi_{PSPI}}{\partial z} = \iint ik_z(x)\psi(x',0)\exp\left(ik_z(x)z - ik_x\left[x - x'\right]\right)dx'dk_x \qquad (13)$$

and

$$\frac{\partial^2 \psi_{PSPI}}{\partial z^2} = \iint -k_z^2(x)\psi(x',0)\exp\left(ik_z(x)z - ik_x\left[x - x'\right]\right)dx'dk_x \qquad (14)$$

then

$$\frac{\partial \psi_{PSPI}}{\partial x} = \iint \left[iz\frac{\partial k_z}{\partial x} - ik_x\right]\psi(x',0)\exp\left(ik_z(x)z - ik_x\left[x - x'\right]\right)dx'dk_x \qquad (15)$$

and

$$\frac{\partial^2 \psi_{PSPI}}{\partial x^2} = \iint \left\{\left[iz\frac{\partial k_z}{\partial x} - ik_x\right]^2 + iz\frac{\partial^2 k_z}{\partial x^2}\right\}\psi(x',0)\exp\left(ik_z(x)z - ik_x\left[x - x'\right]\right)dx'dk_x \qquad (16)$$

which becomes

$$\frac{\partial^2 \psi_{PSPI}}{\partial x^2} =$$
$$\iint \left[-k_x^2 + 2k_x z\frac{\partial k_z}{\partial x} - \left(z\frac{\partial k_z}{\partial x}\right)^2 + iz\frac{\partial^2 k_z}{\partial x^2}\right]\psi(x',0)\exp\left(ik_z(x)z - ik_x\left[x - x'\right]\right)dx'dk_x \qquad (17)$$

The wave equation requires the sum of equations (14) and (17)

$$\frac{\partial^2 \psi_{PSPI}}{\partial z^2} + \frac{\partial^2 \psi_{PSPI}}{\partial x^2} =$$
$$\iint \left[-k_z^2 - k_x^2 + 2k_x z\frac{\partial k_z}{\partial x} - \left(z\frac{\partial k_z}{\partial x}\right)^2 + iz\frac{\partial^2 k_z}{\partial x^2}\right]\psi(x',0)\exp\left(ik_z(x)z - ik_x\left[x - x'\right]\right)dx'dk_x \qquad (18)$$

which is

$$\frac{\partial^2\psi_{PSPI}}{\partial z^2}+\frac{\partial^2\psi_{PSPI}}{\partial x^2}=-\frac{\omega^2}{v^2(x)}\psi_{PSPI}+$$
$$\iint\left[2ik_x z\frac{\partial k_z}{\partial x}-\left(z\frac{\partial k_z}{\partial x}\right)^2+iz\frac{\partial^2 k_z}{\partial x^2}\right]\psi(x',0)\exp\left(ik_z(x)z-ik_x\left[x-x'\right]\right)dx'dk_x \qquad (19)$$

The double integral on the right-hand-side of equation (19) represents the error term of PSPI. Note that it will vanish for constant velocity as all terms contain velocity gradients through $\partial k_z/\partial x$.

NSPS formulae

For NSPS, the z derivative works similarly but the x derivative is much simpler because k_z does not depend on x.

$$\frac{\partial^2\psi_{NSPS}}{\partial z^2}=\iint -k_z^2(x')\psi(x',0)\exp\left(ik_z(x')z-ik_x\left[x-x'\right]\right)dx'dk_x \qquad (20)$$

and

$$\frac{\partial^2\psi_{NSPS}}{\partial x^2}=\iint -k_x^2\psi(x',0)\exp\left(ik_z(x')z-ik_x\left[x-x'\right]\right)dx'dk_x \qquad (21)$$

So the sum of (20) and (21) gives

$$\frac{\partial^2\psi_{NSPS}}{\partial z^2}+\frac{\partial^2\psi_{NSPS}}{\partial x^2}=\iint\left[-k_z^2(x')-k_x^2\right]\psi(x',0)\exp\left(ik_z(x')z-ik_x\left[x-x'\right]\right)dx'dk_x \qquad (22)$$

or

$$\frac{\partial^2\psi_{NSPS}}{\partial z^2}+\frac{\partial^2\psi_{NSPS}}{\partial x^2}=\iint -\frac{\omega^2}{v^2(x')}\psi(x',0)\exp\left(ik_z(x')z-ik_x\left[x-x'\right]\right)dx'dk_x \qquad (23)$$

which can be rewritten as

$$\frac{\partial^2\psi_{NSPS}}{\partial z^2}+\frac{\partial^2\psi_{NSPS}}{\partial x^2}=-\frac{\omega^2}{v^2(x)}\psi_{NSPS}+$$
$$\iint\left[\frac{\omega^2}{v^2(x)}-\frac{\omega^2}{v^2(x')}\right]\psi(x',0)\exp\left(ik_z(x')z-ik_x\left[x-x'\right]\right)dx'dk_x \qquad (24)$$

The NSPS error term is also a double integral but of significantly different character than that for PSPI. Note the absence of explicit velocity derivatives. This error term also vanishes identically for constant velocity.

In a sense, equation (23) shows that NSPS relates the Laplacian at finite z to the NSPS extrapolation of the Laplacian at z=0. Thus, we expect the error term in NSPS to depend on the size of the depth step more strongly than the velocity gradient.

PROOF OF ADJOINT RELATIONSHIP

A wavefield extrapolation operator is an example of a member of the abstract class of linear mathematical operators. The concept of an adjoint operator is fundamental to the study of the behavior of abstract operators because operators that are self-adjoint (also called Hermetian) can be shown to have a complete set of orthogonal eigenvectors and real eigenvalues. This means that a self-adjoint operator, L_H, can always be decomposed as $L_H=U\Lambda U^H$ where U^H is the Hermetian conjugate (i.e. complex-conjugate transpose) of U, U is a unitary matrix ($U^HU=UU^H=1$), and Λ is a diagonal matrix of eigenvalues, λ. If none of the λ's vanish, then $L_H^{-1}=U\Lambda^{-1}U^H$ and the inverse is easily calculated. Furthermore, Wapenaar and Grimbergen (1998) show that the stability requirement for self-adjoint operators is simply $|\lambda|<1$.

If we let L_P be the linear operator that accomplishes PSPI and L_N be a similar operator for NSPS, then we can write these processes as

$$\psi(x,z)_{PSPI} = \iint \psi_0(x')\alpha(k_x,x,z)\exp\left(ik_x[x'-x]\right)dx'dk_x \equiv L_P\psi_0 \tag{25}$$

and

$$\psi(x,z)_{NSPS} = \iint \psi_0(x')\alpha(k_x,x',z)\exp\left(ik_x[x'-x]\right)dx'dk_x \equiv L_N\psi_0 . \tag{26}$$

If L is any linear operator, then the adjoint of L, L^A is defined by (Stein, 1993)

$$\left\langle L\psi_0,\psi_1\right\rangle = \left\langle \psi_0,L^A\psi_1\right\rangle \tag{27}$$

where < > defines an inner product integral given by

$$\left\langle \psi_m,\psi_n\right\rangle \equiv \int \psi_m(x)\psi_n^*(x)dx \tag{28}$$

and * indicates complex conjugation. Using these expressions, the adjoint operator for L_P must satisfy

$$\left\langle L_P\psi_0,\psi_1\right\rangle = \left\langle \psi_0,L_P^A\psi_1\right\rangle . \tag{29}$$

Using equation (25) the bracket on the left-hand-side of equation (29) expands as

$$\left\langle L_P\psi_0,\psi_1\right\rangle = \int \psi_1^*(x)\left[\iint \psi_0(x')\alpha(k_x,x,z)\exp\left(ik_x[x'-x]\right)dx'dk_x\right]dx . \tag{30}$$

Upon interchanging the order of x and x' integrations this can be manipulated into

$$\left\langle L_P\psi_0,\psi_1\right\rangle = \int \psi_0(x')\left[\iint \psi_1(x)\alpha^*(k_x,x,z)\exp\left(ik_x[x-x']\right)dxdk_x\right]^* dx' . \tag{31}$$

The expression in square brackets should be compared to equation (26) which shows it to be an NSPS operation using the complex-conjugate extrapolator. Inspection of

equation (5) shows that complex conjugation is equivalent to reversing the sign on "z" which means the direction of extrapolation is changed. Using + and – subscripts to indicate the direction of extrapolation, the desired adjoint of L_P is then

$$L^{A}_{P+} = L_{N-} \tag{32}$$

Thus the adjoint process to PSPI is NSPS in the opposite direction and vice-versa.

THE COMBINED EXTRAPOLATOR

The preceding analyses all suggest a complementary relationship between NSPS and PSPI so it seems natural to try to combine them into a single downward continuation process. As motivation, observe that NSPS has the physical interpretation (Figure 4a) of wavefield propagation by "emission" from the upper datum while PSPI (Figure 4b) has the interpretation of extrapolation by "reception". In other words, NSPS "pushes out" a Huygen's wavefield from each input point using the local velocities at the input location while PSPI "pulls in" wavefield energy to each output point using the local velocities at that output location. A combined process is suggested in Figure 4c where the first half of the extrapolation is done with NSPS and the second half with PSPI. This new method will be called *symmetric nonstationary phase shift* or SNPS.

Comparison of equations (3) and (6) shows that the desired SNPS form can be derived by substituting (6) into (3) with z/2 replacing z in each extrapolator and taking care to separate input and output coordinates. This leads to

$$\psi(x,z)_{SNPS} = \int \left[\int \psi(x',0)\alpha(k_x,x',z/2)\exp(ik_x x')dx' \right] \alpha(k_x,x,z/2)\exp(-ik_x x)dk_x \tag{33}$$

where

$$\alpha(k_x,x,z/2) = \exp\left(i\frac{z}{2}\sqrt{\frac{\omega^2}{v(x)^2} - k_x^2} \right) = \alpha(k_x,x,z)^{1/2} \tag{34}$$

and a similar expression for $\alpha(k_x,x',z/2)$. The apparent complexity of equation (33) can be lessened by incorporating both extrapolators into a single term

$$\psi(x,z)_{SNPS} = \int \psi(x',0)\Delta(x',x,z)dx' \tag{35}$$

where

$$\Delta(x',x,z) = \int \alpha(k_x,x',z/2)\,\alpha(k_x,x,z/2)\exp\left(ik_x(x'-x)\right)dk_x \tag{36}$$

is the combined extrapolator in the space domain. Equation (34) becomes a matrix-vector multiplication for discretely sampled data and equation (35) is an explicit expression for the extrapolation matrix. For completeness and ease of comparison, we present the alternate forms of $\Delta(x',x,z)$ for the other algorithms. For NSPS, both α's

in the integrand are given x′ dependence and they combine into a single extrapolator to give

$$\Delta\left(x',x,z\right)_{NSPS} = \int \alpha\left(k_x,x',z\right)\exp\left(ik_x\left(x'-x\right)\right)dk_x. \tag{37}$$

For PSPI, a similar result is obtained except the α dependence is on x

$$\Delta\left(x',x,z\right)_{PSPI} = \int \alpha\left(k_x,x,z\right)\exp\left(ik_x\left(x'-x\right)\right)dk_x. \tag{38}$$

In the case of simple constant velocity phase-shift, both α's lose their x dependence entirely and the result is

$$\Delta\left(x',x,z\right)_{PS} = \int \alpha\left(k_x,z\right)\exp\left(ik_x\left(x'-x\right)\right)dk_x. \tag{39}$$

Comparison of equations (36) through (39) reveals an important point: only the SNPS extrapolator (equation 36) and the constant velocity result (equation 39) are symmetric under the exchange of x and x′ (this assumes that velocity is independent of z so that v(x,z)=v(x,0)). According to Wapenaar and Grimbergen (1998) this symmetry is required by reciprocity. The proof for equation (36) simply requires the exchange of x and x′ and then a replacement of k_x by $-k_x$. Since α depends on the square of k_x, this last step merely absorbs the sign change in the complex exponential that is caused by the variable exchange. Though the SNPS and PS operators are symmetric, they are not self-adjoint.

An alternate viewpoint follows from the windowing analog. In this case, SNPS becomes

$$\psi\left(x,z\right)_{SNPS} = \sum_j \left\{ \Omega_j \mathbf{IFT}_{k_x \Rightarrow x} \left(\alpha_j^{1/2} \sum_n \left[\alpha'^{1/2}_n \mathbf{FT}_{x' \Rightarrow k_x} \left(\Omega'_n \psi\left(x',0\right)\right)\right]\right)\right\}. \tag{40}$$

In this expression, primes are used to distinguish quantities dependent on input coordinates and $\alpha_j^{1/2}$ is the extrapolator of equation (34) evaluated for the constant velocity v_j. This expression makes clear the splitting of the extrapolation operator into an operation on input and another on output, which gives intuitive basis to its symmetry.

STABILITY ANALYSIS

Etgen (1994), Dellinger and Etgen (1996), and Wapenaar and Grimbergen (1998) all made important contributions to the stability analysis of explicit extrapolation operators. Etgen showed an explicit numerical example of instability and used SVD (singular value decomposition) to relate the occurrence of instability to singular values of magnitude greater than unity. If L is a discrete extrapolation matrix, then its SVD is

$$L = USV^H \tag{41}$$

where U is composed of the eigenvectors of LL^H, V is built form the eigenvectors of L^HL, both U and V are unitary (e.g. $UU^H=U^HU=I$ and similarly for V), and S is a diagonal matrix containing the non-negative singular values, s.

According to Wapenaar and Grimbergen, an extrapolation operator is unconditionally stable if, for any vector ψ,

$$\|L\psi\| \le \|\psi\| \tag{42}$$

where the double vertical bars indicate a norm. Substitution of equation (41) in (42) gives

$$\|L\psi\| = \|USV^H\psi\| \le \|U\|\|S\|\|V^H\|\|\psi\| = \max(s)\|\psi\| \le \|\psi\| \tag{43}$$

The last expression, which follows because the norm of a unitary matrix is 1 and the norm of a diagonal matrix is its largest absolute value (Strang, 1993, p384), gives the stability condition. Thus, for complete stability, the largest singular value must be less than one. It is easily shown that the PS extrapolator (equation 39) is unconditionally stable.

We do not yet have a complete, analytic, stability analysis of the operators prescribed by equations (36) through (39) so we will follow Etgen and present a numerical study using SVD software. Figure 5 shows a velocity model similar to the Etgen model that we will use for this analysis. Figure 6 shows the singular values of NSPS, PSPI, and SNPS for a monochromatic extrapolation (25 Hz) over a 30 m vertical step through the sediment column model of Figure 5. This and the following simulations all used a horizontal spatial sample rate of 30m. Many of the singular values are precisely unity but a few are greater which indicates the instability noticed by Etgen. The decay of values numbered above 40 is due to evanescent energy. PSPI and NSPS show nearly identical instability while SNPS is somewhat better.

A simple strategy to improve stability is to make the extrapolation operators slightly dissipative. (This is a practical approach that does not address the theoretical reasons for the problem in the first place.) Dissipation is introduced by giving the velocity function a small complex part. That is v(x) is replaced by $v_c(x)=v(x)+i\eta v(x)$ where η is a small number on the order of .01 . This can be shown to introduce attenuation that increases with traveltime. (In the theory of visco-elasticity, the *visco-elastic correspondence principle* states that any elastic theory can be made visco-elastic by formulating it in the frequency domain with complex-valued elastic parameters.) Then, $\alpha(k_x,x,z)$ is computed as

$$\alpha(k_x,x,z) = \exp\left(iz\,\mathrm{real}(k_z) - \left|z\,\mathrm{imag}(k_z)\right|\right) \tag{44}$$

where

$$k_z = \sqrt{\frac{\omega^2}{v_c(x)^2} - k_x^2} \tag{45}$$

Figure 7 shows a repetition of the experiment of Figure 6 with the complex velocity factor, η, set to .03. The immediate effect is to reduce all of the singular values. NSPS and PSPI still have some instability while SNPS has become completely stable. However, this is not a general proof of stability and a similar calculation for 50 Hz (Figure 8) and 12.5 Hz (Figure 9) reveals that lower frequencies are less stable than higher frequencies.

The foregoing suggests that the stability question is multifaceted. A more complete investigation, but which is still dependent on a single assumed velocity model, is shown in Figures 10 through 13. Figure 10 shows the largest singular value from each of a series of tests like those shown in the previous figures. Here, the dz step was fixed at 30m and frequency at 12.5 Hz and the percentage of imaginary velocity, 100η, was varied from 0 to 10%. NSPS and PSPI did not become fully stable until 4% while SNPS stabilized earlier at just above 2%.

In Figure 11, η was fixed at .03 (3%) and frequency again at 25 Hz while the dz step was varied from 0 to 150 m. NSPS and PSPI were unstable for dz steps less than 70m while SNPS was stable for the entire range. The reason for the increasing stability with increasing step size is probably that the numerical attenuation has progressively greater effects.

Figures 12 and 13 are two different studies of the frequency dependence of the instability. Both figures had η of .03 and Figure 12 shows results for a dz step of 25 m while Figure 13 is for a dz of 75m. Again SNPS is much more stable than the other two algorithms. The oscillations of the SNPS curve are noteworthy but we offer no explanation.

Finally, Figures 14 through 21 show the results of a wavefield extrapolation experiment using NSPS, PSPI, and SNPS extrapolators. In each case, twenty extrapolation steps were taken through the “sediment column” model (marked “a” in Figure 5) and a further twenty through a homogeneous sediment layer (marked “b” in Figure 5). The extrapolators were run with η of .03 and a dz step of 30m.

Figure 14 shows the NSPS result after twenty 30m steps through the sediment column velocity model. The delayed central portion of the wavefield is clearly evident in 14a as are other “diffraction” events associated with the column. The clearly defined evanescent boundary in 14b corresponds to the fast salt velocity while the slight energy outside this is not evanescent leakage (as with PSPI) but is wavefield energy in the slower sediment column. Figure 15 shows the wavefield of Figure 14 after a further twenty steps through a homogeneous layer beneath the salt. The decrease in energy at higher wavenumbers and frequencies is due to wavefront spreading.

Figures 16 and 17 were generated with PSPI and compare directly with Figures 14 and 15 respectively. PSPI shows slight evanescent leakage and slightly different character in the sediment column (compare Figures 16 and 14).

Figures 18 and 19 were generated with SNPS. Figure 18 compares with Figures 14 and 16 while Figure 19 compares with 15 and 17.

It is difficult to discern any visual evidence of instability in these figures. The instability caused by a singular value of 1.05 over twenty steps grows to only 1.05^{20} or about 2.7. Differences between all of these figures are subtle so their numerical differences are displayed in Figures 20 and 21. Figure 20 shows differences between the results after twenty steps through the sediment column model while Figure 21 shows differences between the results after a further twenty steps in the homogeneous model. In each figure a) and b) are the difference between SNPS and NSPS or PSPI respectively. These appear to be roughly reverse polarity versions of one another. The differences between PSPI and NSPS are in c) and are the largest in each case. For interest, d) shows the difference between SNPS and the average of NSPS and PSPI. The smallness of this result indicates that SNPS is somewhere between NSPS and PSPI in behavior but is not simply their average. It is also interesting to note that the differences between the algorithms, though generated solely by the sediment column, persist into the homogeneous layer and seem to become stronger.

CONCLUSIONS

The NSPS and PSPI wavefield extrapolators are fundamentally complementary. NSPS "pushes out" a wavefield from its initial position while PSPI pulls the wavefield into its final position. Both can be used as one-way wavefield extrapolators to construct approximate solutions to the variable-velocity wave equation, though the error terms are distinctly different.

A formal mathematical proof shows that extrapolation with NSPS in a direction orthogonal to the velocity gradient is the adjoint process to extrapolation with PSPI in the opposite direction. Thus neither process is self-adjoint.

NSPS and PSPI can be combined into a *symmetric nonstationary phase shift* (SNPS) extrapolator. This new extrapolator has the symmetry required by reciprocity which both NSPS and PSPI lack.

SVD based stability analysis shows the SNPS extrapolator to have a much greater stability range than either NSPS or PSPI. The stability of all three algorithms is enhanced by giving the velocity a small imaginary part. This results in a natural attenuation that increases with traveltime and frequency. Stability is shown to be a complex issue that depends upon velocity gradient, dz step, and frequency.

Numerical experimentation shows visually similar results from all three extrapolators. Detailed examination shows that NSPS and PSPI are the most dissimilar while SNPS falls somewhere in between.

We note that other symmetric extrapolators are possible. Another simple one would use PSPI first and then NSPS. It seems likely that the stability question will also depend on the vertical velocity gradient and that effect was not considered. Vertical velocity variations will break the symmetry of the SNPS extrapolator presented here. However, a symmetric process is still possible by prescribing the velocity function midway between the initial and final depths. Then, for example, PSPI could pull the wavefield into the center where NSPS pushes it out with full velocity symmetry.

REFERENCES

Berkhout, A.J., 1985, Seismic Migration: Imaging of acoustic energy by wavefield extrapolation: in Developments in Solid Earth Geophysics, **14A**, Elsevier.

Claerbout, J, 1976, Fundamentals of Geophysical Data Processing: McGraw-Hill.

Dellinger, J., and Etgen, J.T., 1996, Eigenvalues, singular values, and stability analysis: Expanded abstracts 66th SEG International Convention, 1975-1978.

Etgen, J.T., 1994, Stability analysis of explicit depth extrapolation through laterally-varying media: Expanded abstracts 64th SEG International Convention, 1266-1269.

Gazdag, J., 1978, Wave-equation migration by phase shift: Geophysics, **43**, 1342-1351.

Gazdag, J., and Squazerro, P., 1984, Migration of seismic data by phase shift plus interpolation: Geophysics, **49**, 124-131.

Grimbergen, J.L.T., Dessing, F.J., and Wapenaar, C.P.A, 1998, Modal expansion of one-way operators in laterally varying media: Geophysics, **63**, 995-1005.

Margrave, G.F., 1998, Theory of nonstationary linear filtering in the Fourier domain with application to time-variant filtering: Geophysics, **63**, 244-259.

Margrave and Ferguson, 1997, Wavefield extrapolation by nonstationary phase shift: Expanded abstracts 1997 SEG International Convention, and 9th Annual Research Report of the CREWES Project.

Strang, G., 1993, Introduction to linear Algebra: Wellesley-Cambridge Press, ISBN 0-9614088-2-0.

Wapenaar, K, and Grimbergen, J.L.T., 1998, A discussion on stability analysis of wavefield depth extrapolation: Expanded abstracts 68th SEG International Convention, 1716-1719.

ACKNOWLEDGEMENTS

We thank the Sponsors of the CREWES Project for their generous support.

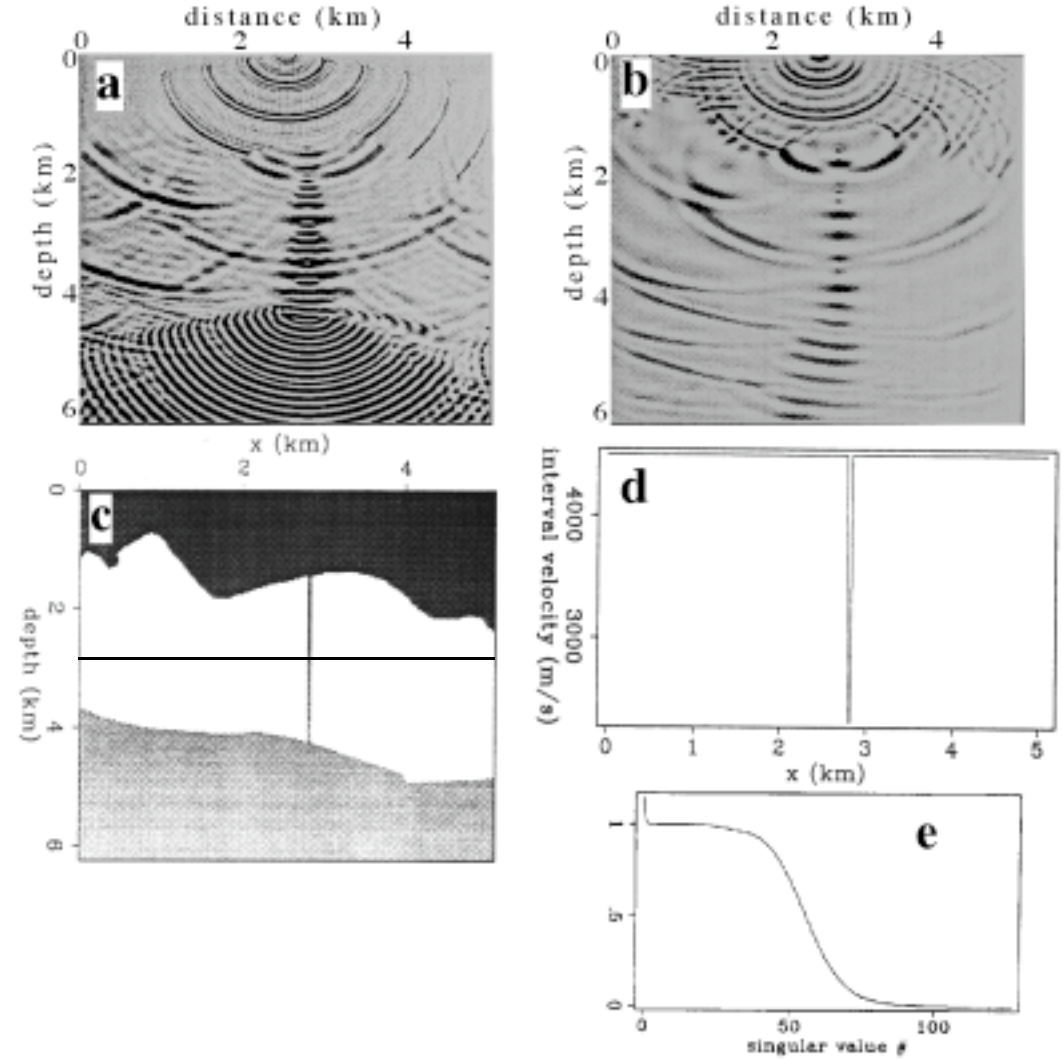

Fig. 1. An example of unstable explicit wavefield extrapolation taken from Etgen (1994). a) An ω-x migration (designed to simulate PSPI) which shows an unstable amplitude growth, b) A reverse-time migration which produces a stable result, c) the velocity model used for (a) and (b). The salt layer (white) has an artificial "sediment column" that causes the instability. d) A profile through the velocity model (along the horizontal line in c) showing the velocity contrast across the sediment column. e) The singular values for an ω-x extrapolation through the sediment column. Values greater than unity indicate instability.

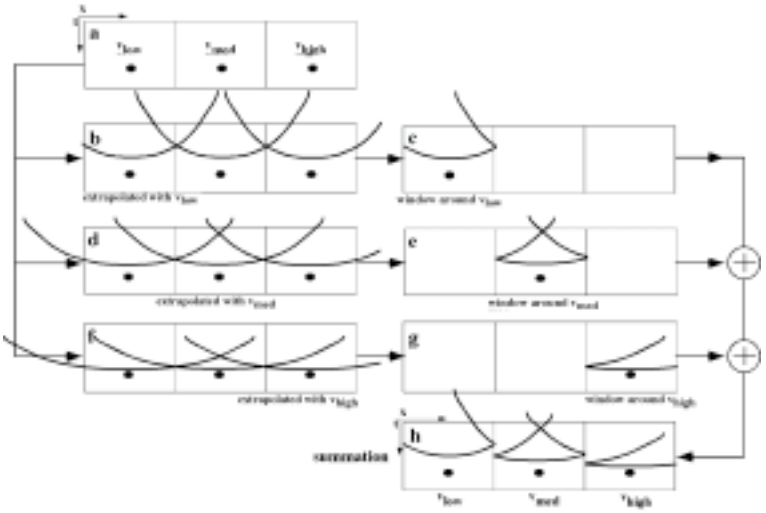

Figure 2. Wavefield extrapolation by nonstationary combination is depicted. The input wavefield (a) consists of 3 impulses in three distinct velocity regions. The first computation step is a complete wavefield extrapolation of the input for each distinct velocity (b), (c), and (d). Next, a boxcar window is applied to each extrapolation which zeros all locations where a particular velocity was not the correct one (e), (f), (g). In the final step, the extrapolated-windowed wavefields are superimposed (h). Note the wavefield discontinuities produced at the velocity boundaries.

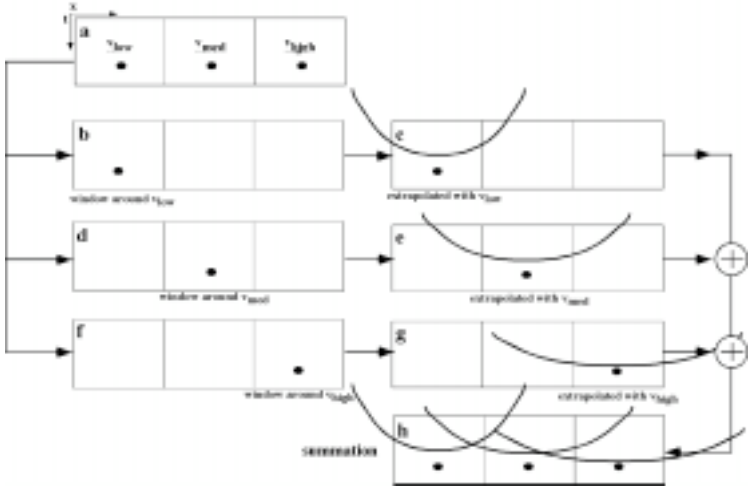

Figure 3. Wavefield extrapolation by nonstationary convolution is depicted. The computation reverses the operations of windowing and extrapolation as described nor nonstationary combination (Figure 3). The first computation step windows the input wavefield into three distinct regions which isolated each impulse (b), (c), (d). Next, each windowed wavefield is extrapolated with the appropriate constant velocity(e), (f), (g). In the final step, the extrapolated-windowed wavefields are superimposed (h). The result is a superposition of impulse responses.

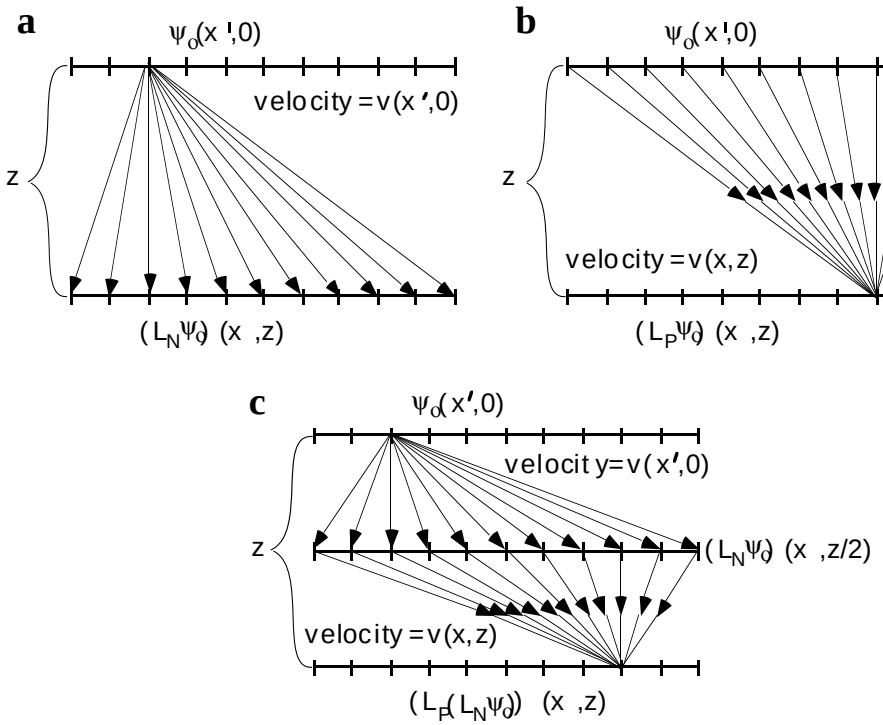

Fig. 4. Conceptual descriptions of the explicit extrapolators discussed in the text. In each case a wavefield is extrapolated from depth 0 to depth z. a) The NSPS extrapolator "pushes out" the wavefield from the starting datum. The extrapolator is locally similar to stationary phase shift using the velocity field v(x′,0). b) The PSPI extrapolator "pulls in" the wavefield to the ending datum. The extrapolator is locally similar to stationary phase shift using the velocity field v(x,z). c) The SNPS extrapolator uses the NSPS approach to go half-way and then uses PSPI for the second half-step.

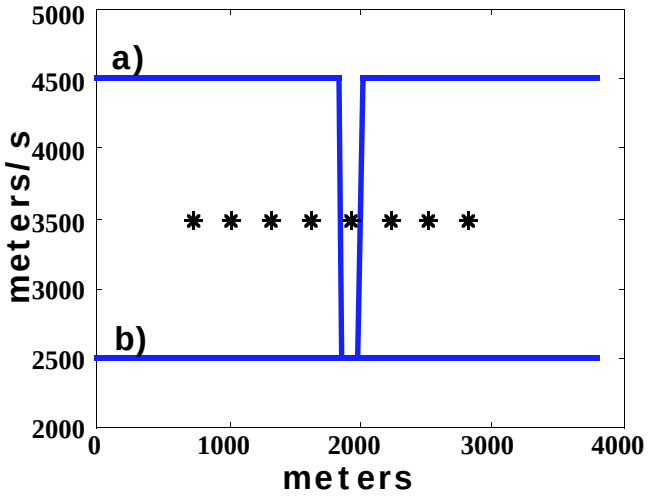

Fig. 5. The velocity model used in the stability simulations. The upper curve a) is similar to Etgen's "sediment column" model (see Figure 1) while the lower line b) represents a homogeneous medium below the sediment column model. Stars mark the x location of impulses input into the wavefield extrapolation tests of Figures 14 through 19.

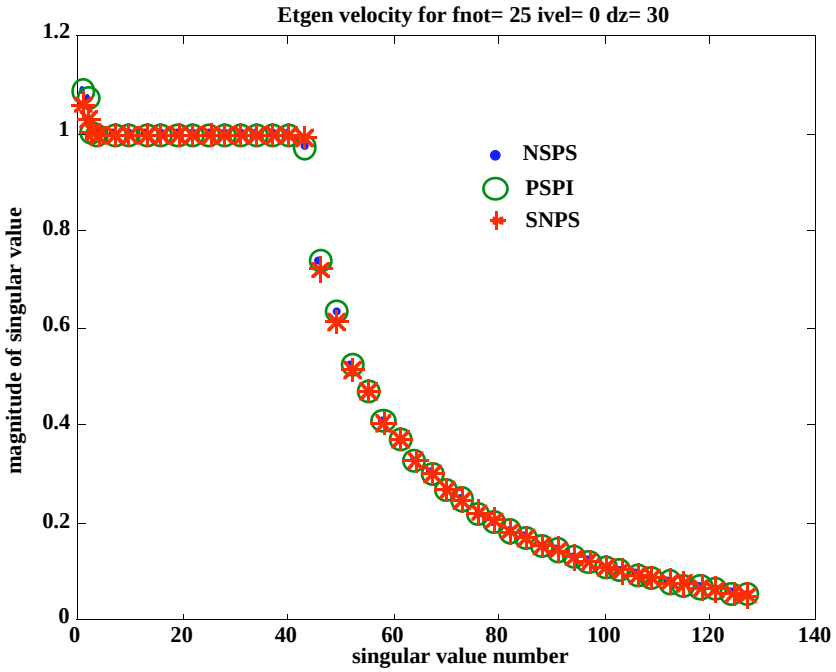

Fig. 6. The singular values for the three extrapolators discussed in the text for a 30m dz step at 25 Hz. The spatial sample rate was also 30m. Note that all three show evidence of instability but the effect is markedly better for SNPS. The velocity field was that of Figure 5 and was purely real.

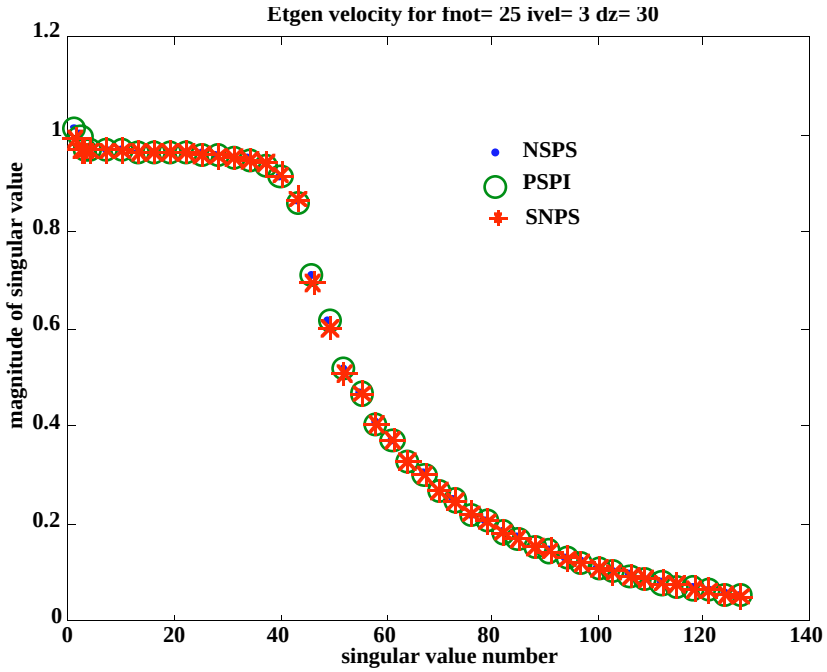

Fig. 7. The singular values for NSPS, PSPI, and SNPS are shown for the same case as in Figure 6 except that the velocity function was given an imaginary component of 3% of the real part. The result is a numerical attenuation which drives the algorithms towards stability. Note that SNPS has become completely stable (i.e. no singular values greater than unity).

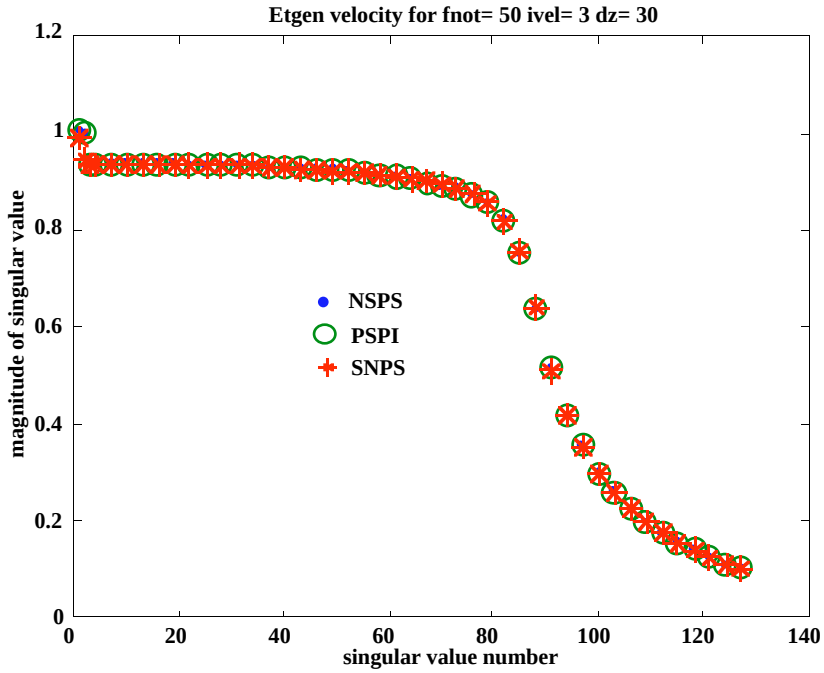

Fig. 8. The singular values for NSPS, PSPI, and SNPS are shown for the same case as in Figure 7 except that the frequency has been doubled to 50 Hz. Compared with Figure 7, this result shows greater stability for all three algorithms.

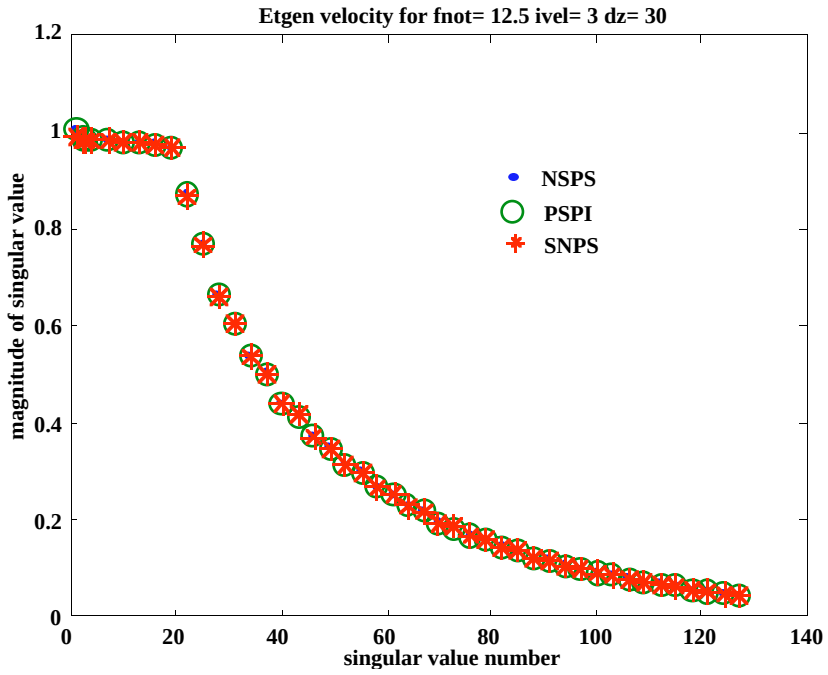

Fig. 9. The singular values for NSPS, PSPI, and SNPS are shown for the same case as in Figure 7 except that the frequency has been halved to 12.5 Hz. Compared with Figure 7, this result shows similar (but slightly less) stability for all three algorithms.

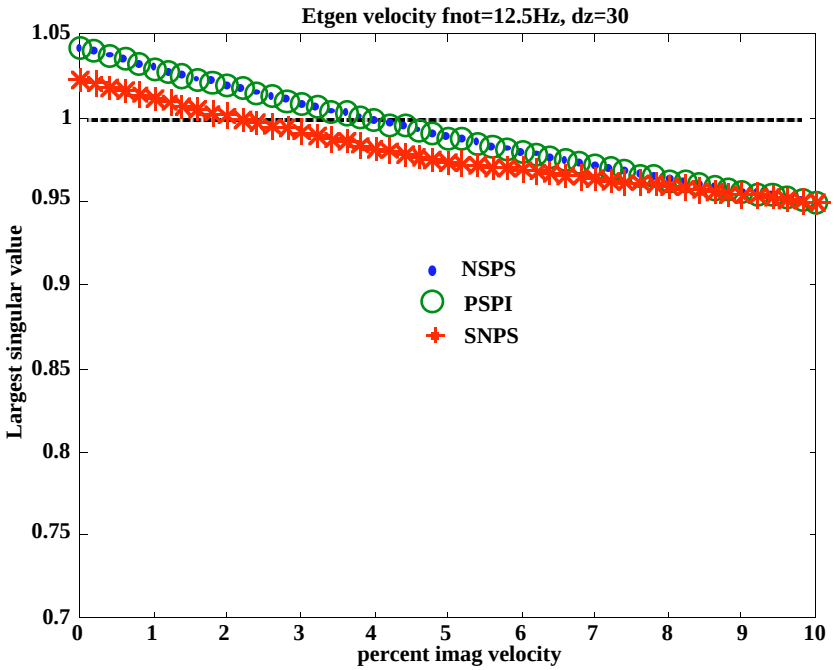

Fig. 10. The largest singular value is shown for each of NSPS, PSPI, and SNPS for the velocity model of Figure 5a, a step size of 30m, a frequency of 12.5 Hz, versus a range of imaginary velocity percentages. PSPI and NSPS show exactly the same degree of instability while SNPS stabilizes earlier.

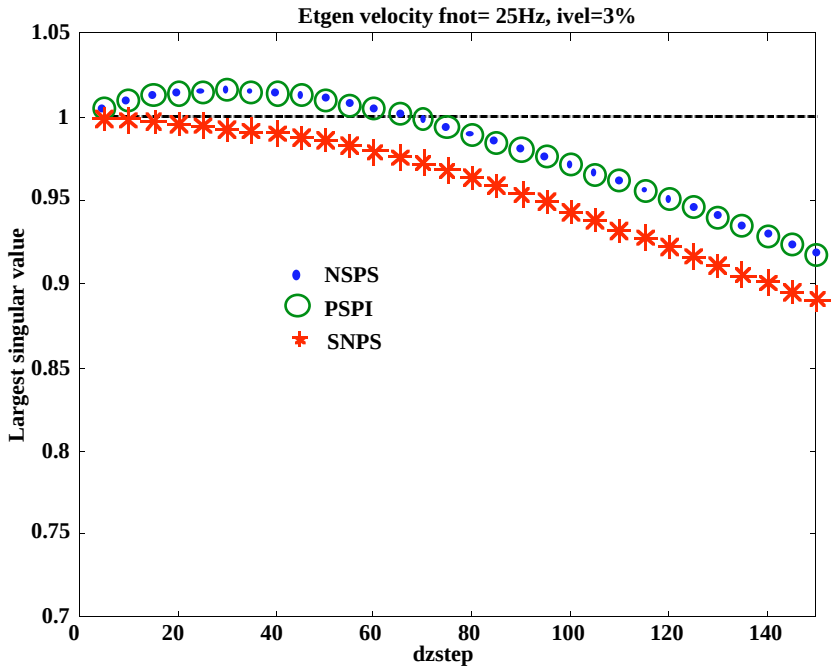

Fig. 11. The largest singular value is shown for each of NSPS, PSPI, and SNPS for the velocity model of Figure 5a, a frequency of 25 Hz, and imaginary velocity of 3%, versus a range of extrapolation step sizes. PSPI and NSPS are unstable until a 70m step is reached while SNPS is always stable.

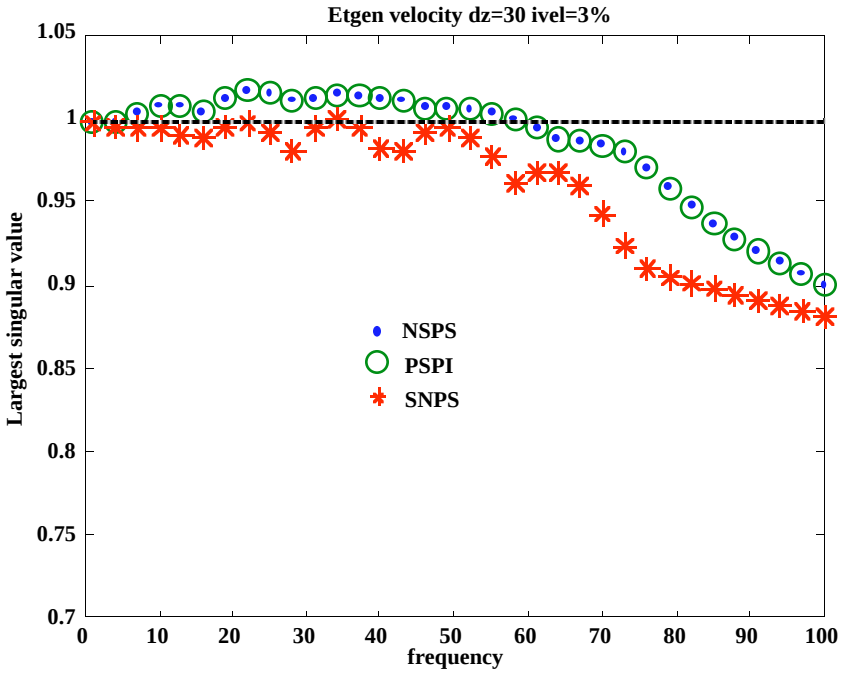

Fig. 12. The largest singular value is shown for each of NSPS, PSPI, and SNPS for the velocity model of Figure 5a, a step size of 30m, and imaginary velocity of 3%, versus a range of frequencies. PSPI and NSPS are unstable until 60 Hz while SNPS is almost always stable. The cause of the oscillations in the SNPS curve is unknown.

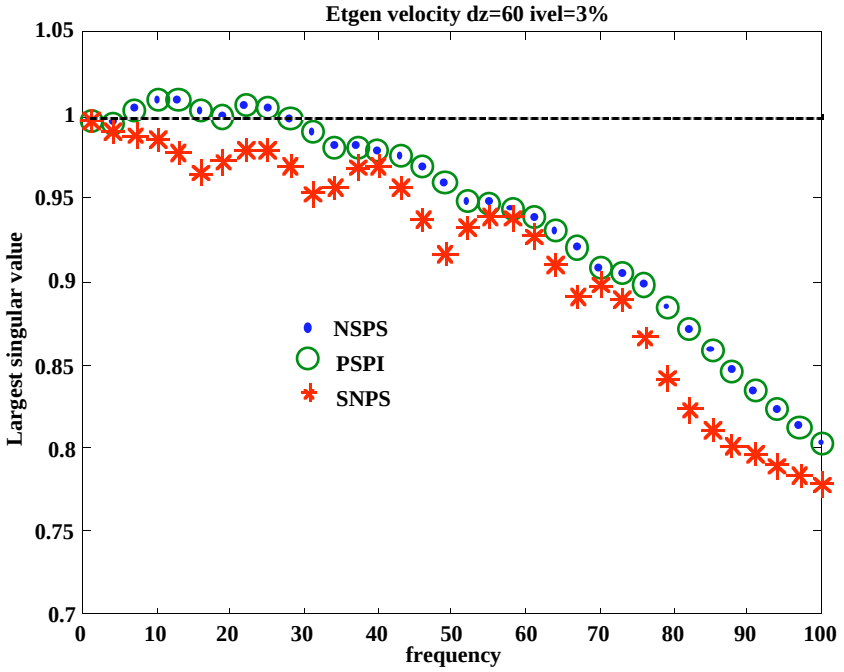

Fig. 13. A repeat of the study of Figure 12 but the step size has been doubled to 60m. Stability of all algorithms has increased because the numerical attenuation increases with traveltime. PSPI and NSPS are unstable until 30 Hz while SNPS is always stable. The cause of the oscillations in the curves is unknown.

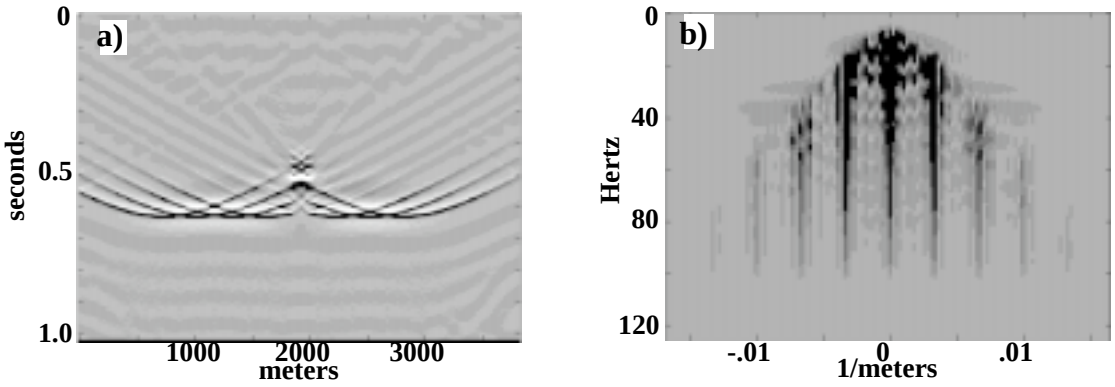

Figure 14. An extrapolation through the velocity model of Figure 5a. Twenty extrapolation steps of 30m each were taken with NSPS using 3% imaginary velocities. The time domain result is in a) and the f-k spectrum in b). The input wavefield had eight impulses at positions shown on Figure 5.

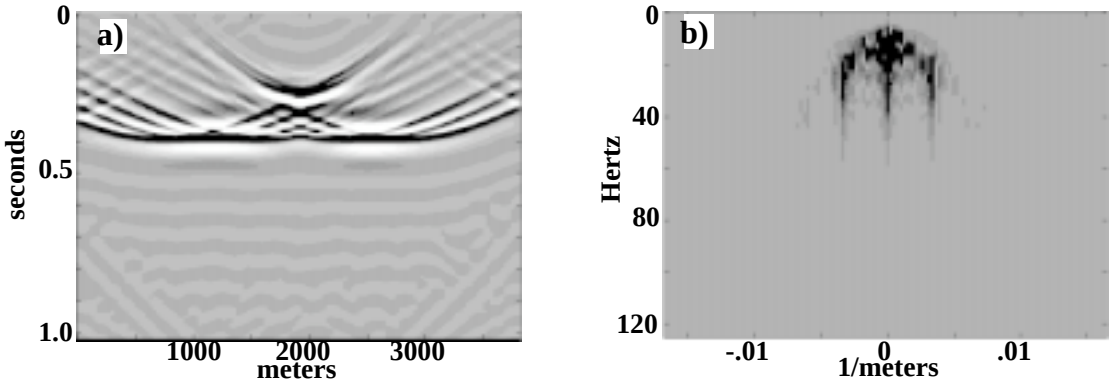

Figure 15. An extrapolation of the dataset in Figure 14 through the velocity model of Figure 5b. Twenty extrapolation steps of 30m each were taken with NSPS using 3% imaginary velocities. The time domain result is in a) and the f-k spectrum in b).

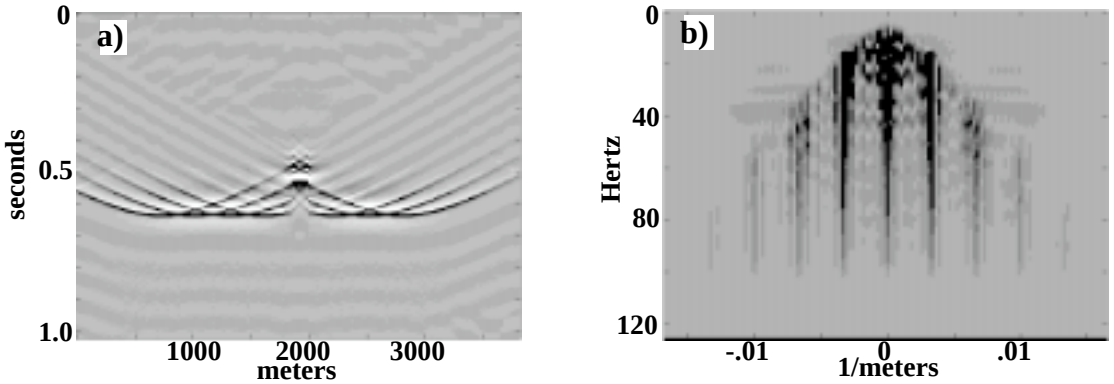

Figure 16. An extrapolation through the velocity model of Figure 5a. Twenty extrapolation steps of 30m each were taken with PSPI using 3% imaginary velocities. The time domain result is in a) and the f-k spectrum in b). The input wavefield had eight impulses at positions shown on Figure 5.

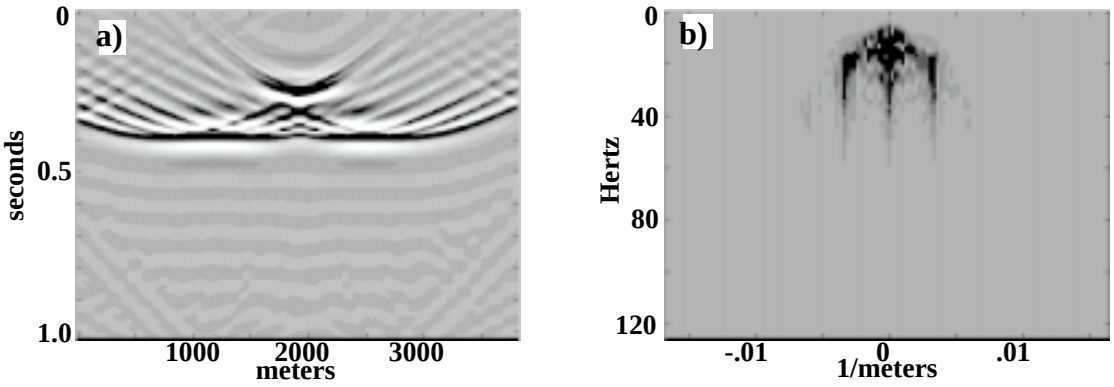

Figure 17. An extrapolation of the dataset in Figure 16 through the velocity model of Figure 5b. Twenty extrapolation steps of 30m each were taken with PSPI using 3% imaginary velocities. The time domain result is in a) and the f-k spectrum in b).

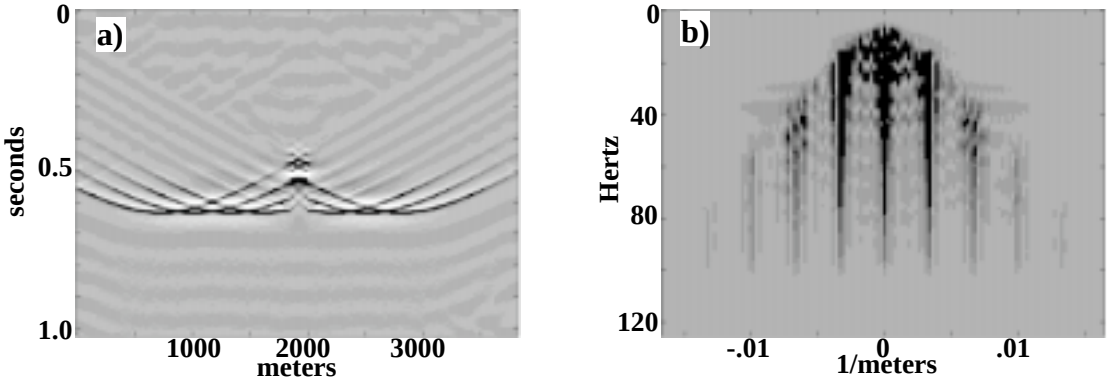

Figure 18. An extrapolation through the velocity model of Figure 5a. Twenty extrapolation steps of 30m each were taken with SNPS using 3% imaginary velocities. The time domain result is in a) and the f-k spectrum in b). The input wavefield had eight impulses at positions shown on Figure 5.

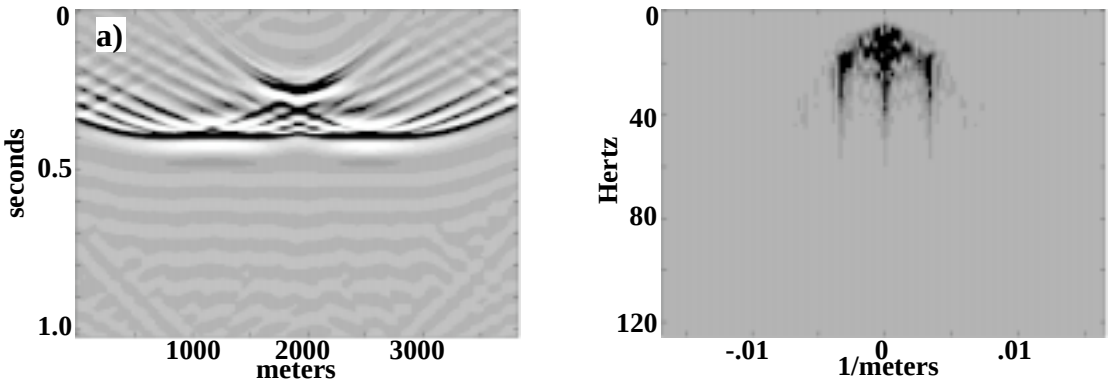

Figure 19. An extrapolation of the dataset in Figure 18 through the velocity model of Figure 5b. Twenty extrapolation steps of 30m each were taken with SNPS using 3% imaginary velocities. The time domain result is in a) and the f-k spectrum in b).

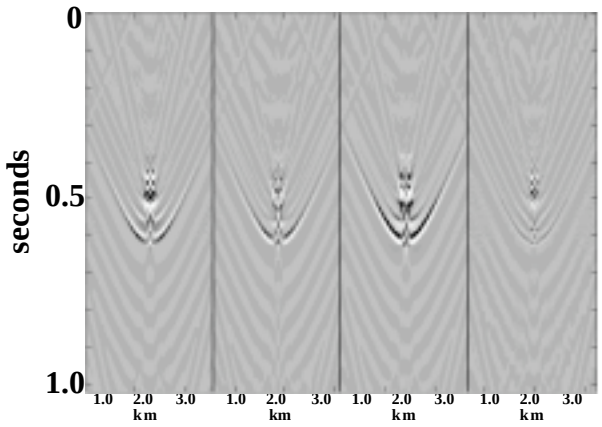

Figure 20. Subtractions of the various wavefield in Figures 14 (NSPS), 16 (PSPI), and 18 (SNPS). a) SNPS - NSPS, b) SNPS - PSPI, c) NSPS - PSPI, d) SNPS - .5(NSPS+PSPI).

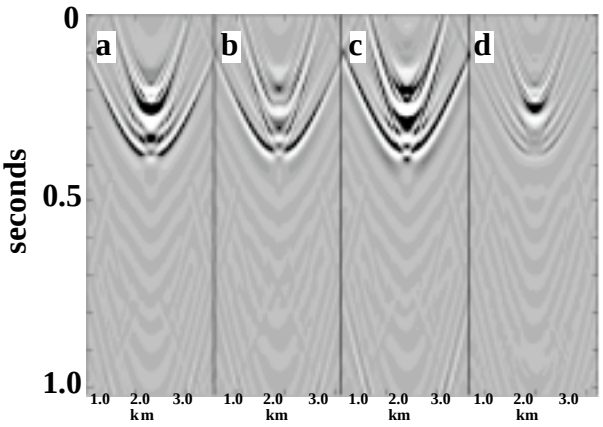

Figure 21. Subtractions of the various wavefield in Figures 15 (NSPS), 17 (PSPI), and 19 (SNPS). a) SNPS - NSPS, b) SNPS - PSPI, c) NSPS - PSPI, d) SNPS - .5(NSPS+PSPI).